Geochemistry Geophysics Geosystems G3
AN ELECTRONIC JOURNAL OF THE EARTH SCIENCES
Published by AGU and the Geochemical Society

Article
Volume 6, Number 11
23 November 2005
Q11010, doi:10.1029/2005GC001027
ISSN: 1525-2027

Crustal structure and rift flank uplift of the Adare Trough, Antarctica

R. Dietmar Müller
School of Geosciences and University of Sydney Institute of Marine Science, University of Sydney, Sydney, NSW 2006, Australia (dietmar@geosci.usyd.edu.au)

Steven C. Cande
Scripps Institution of Oceanography, 9500 Gilman Drive, La Jolla, California 92093, USA

Joann M. Stock
Caltech Seismological Laboratory, Mail Code 252-21, Pasadena, California 91125, USA

William R. Keller
Caltech Seismological Laboratory, Mail Code 252-21, Pasadena, California 91125, USA

Now at Kerr-McGee, 16666 Northchase Drive, Houston, Texas 77040, USA

[1] The Adare Trough, located 100 km northeast of Cape Adare, Antarctica, represents the extinct third arm of a Tertiary spreading ridge between East and West Antarctica. It is characterized by pronounced asymmetric rift flanks elevated up to over 2 km above the trough's basement, accompanied by a large positive mantle Bouguer anomaly. On the basis of recently acquired seismic reflection and ship gravity data, we invert mantle Bouguer anomalies from the Adare Trough and obtain an unexpectedly large oceanic crustal thickness maximum of 9–10.5 km underneath the extinct ridge. A regional positive residual basement depth anomaly between 1 and 2.5 km in amplitude characterizes ocean crust from offshore Victoria Land to the Balleny Islands and north of Iselin Bank. The observations and models indicate that the mid/late Tertiary episode of slow spreading between East and West Antarctica was associated with a mantle thermal anomaly. The increasing crustal thickness toward the extinct ridge indicates that this thermal mantle anomaly may have increased in amplitude through time during the Adare spreading episode. This scenario is supported by a mantle convection model, which indicates the formation and strengthening of a major regional negative upper mantle density anomaly in the southwest Pacific in the last 50 million years. The total amount of post-26 Ma extension associated with Adare Trough normal faulting was about 7.5 km, in anomalously thick oceanic crust with a lithospheric effective elastic thickness (EET) between 3.5 and 5 km. This corresponds to an age between 3 and 5 million years based on a thermal boundary layer model and supports a scenario in which the Adare Trough formed soon after spreading between East and West Antarctica ceased, confined to relatively weak lithosphere with anomalously thick oceanic crust. There is little evidence for major subsequent structural activity in the Adare trough area from the available seismic data, indicating that this part of the West Antarctic Rift system became largely inactive in the early Miocene, with the exception of minor structural reactivation which is visible in the seismic data as offsets up to end of the early Pliocene.

Components: 7368 words, 14 figures, 1 table.

Keywords: Adare Trough; Antarctica; depth anomaly; extinct ridge; flexure; rift.

Index Terms: 0930 Exploration Geophysics: Oceanic structures; 3010 Marine Geology and Geophysics: Gravity and isostasy (1218, 1222); 3035 Marine Geology and Geophysics: Midocean ridge processes.

Received 24 May 2005; **Revised** 23 August 2005; **Accepted** 27 September 2005; **Published** 23 November 2005.

Müller, R. D., S. C. Cande, J. M. Stock, and W. R. Keller (2005), Crustal structure and rift flank uplift of the Adare Trough, Antarctica, *Geochem. Geophys. Geosyst.*, *6*, Q11010, doi:10.1029/2005GC001027.

1. Introduction

[2] The grabens, fracture zones, basement highs and magnetic anomalies on the seafloor north of the Ross Sea (Figures 1, 2, 3, and 4) are among the most important keys to understanding the Cenozoic tectonic development of the West Antarctic Rift System. Figures 2 and 3 illustrate the main tectonic features of the oceanic area to the north of the Ross Sea based on bathymetry and gravity anomalies, including the transition from the shallow Ross Sea to the deep water Adare Basin (Figure 3), the Adare Trough, the Hallett Ridge, and the numerous late Tertiary volcanic cones (see Figure 1 for location of study area). Oceanic magnetic lineations in the Adare Trough and Basin area range from magnetic anomaly 18 to 12 (Figure 4) and suggest the continuation of the oceanic magnetic fabric southward from the Adare Trough to the Adare Basin. The Central Basin east of the Hallett Ridge is characterized by a high-amplitude magnetic anomaly (Figure 4), probably caused by igneous intrusions. By the Oligocene the plate boundary predating the Adare Trough had created a 180 km wide ocean basin north of the Ross Sea, connected to a triple junction among Australia, East, and West Antarctica [*Cande et al.*, 2000].

[3] The Adare Trough is only a well-developed bathymetric feature between 69.5°S and 71°S (Figure 3); further south the extinct axis is buried and/or much smaller in relief (Figure 3). In this paper we focus on the northern, well-developed portion of the Adare Trough. The Adare Trough's topography is highly asymmetric, which may be related to the mapped asymmetry in spreading rates between its east and west flanks (5.5 mm/yr in the west and 7 mm/yr in the east [*Cande et al.*, 2000]) (Figure 3). Linear magnetic anomalies indicate that an extinct ridge is located within the morphologically defined Adare Trough, between magnetic anomalies 12 as outlined in Figure 4. Magnetic anomalies of the Adare Basin can be traced south to about 73°S, suggesting that most of the extension in the Adare Basin continued into the Northern Basin and that the Northern Basin was formed by a combination of crustal thinning and massive, narrowly focused intrusions [*Cande and Stock*, 2005b]. Faulting along the west flank (~1.5 km high) is more pronounced than faulting on the east flank (~1 km high), raising the possibility that faulting of the two flanks was not contemporaneous. Volcanic and igneous activity is known to have occurred in the Western Ross Sea and Marie Byrd Land since around 48 Ma [*Rocchi et al.*, 2002; *Tonarini et al.*, 1997]. This is well expressed in seismic profiles presented in this paper, which highlight the ubiquitous intrusions in the Adare Trough and Basin areas, some of which penetrate the most recent sediments or were the source of extrusive volcanic cones. The primary aim of this study is to determine when faulting occurred and ceased in the Adare Trough area, i.e., whether faulting occurred soon after the cessation of seafloor spreading (i.e., in young lithosphere) or substantially later. Answering this question is crucial for helping to resolve when deformation between East and West Antarctica needs to be considered for closing the global plate circuit. We tackle this problem through combined analysis of seismic reflection data from the RV/IB Nathaniel Palmer and R/V Eltanin and marine gravity anomaly data, which together help constrain a crustal thickness model and a kinematic model for rift-flank uplift.

2. Seismic Data

[4] Our analysis is based on a combination of old and new data from the R/V Eltanin and the RV/IB Nathaniel Palmer (Figure 5). The R/V Eltanin ELT52 seismic line used here is an analog seismic profiler record that was collected in 1972. Seismic line ELT52 intersects DSDP Site 274 on its northern end (Figures 5, 6, and 7) and rises up onto the flank of the Adare Trough to the south where it intersects multichannel seismic lines that were collected during the NBP9702 cruise aboard the RV/IB Nathaniel Palmer. NBP9702 48-channel seismic data were collected at speeds of 5-6 knots with a 1200 m long streamer and six 210 cubic inch GI air guns. Migrated sections along NBP9702 seismic lines A-A′ and B-B′ are shown in Figures 8 and 9. The velocity model used for the migration was generated by semblance velocity analysis. The signal-to-noise ratio on NBP9702 seismic line A-A′ is significantly lower than that of line B-B′ due to rough seas and bad weather. Seismic penetration is typically 1–1.5 seconds

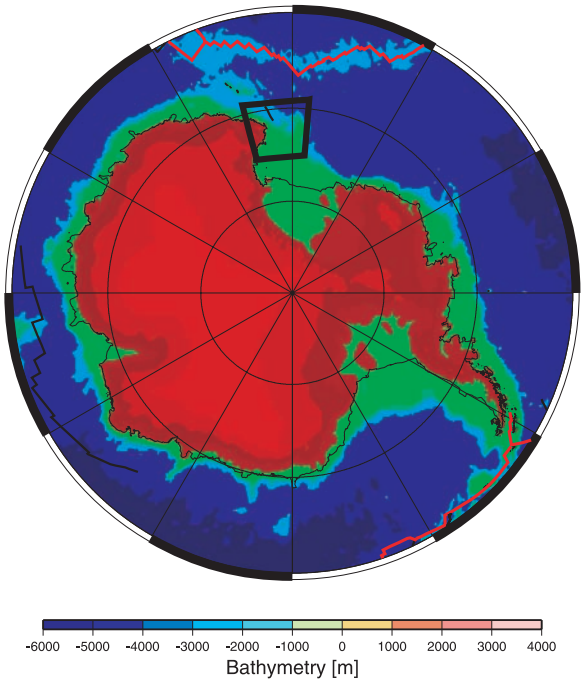

Figure 1. Topography of Antarctica and the circumpolar ocean basins. The Adare Trough area shown in Figure 2 is outlined in bold black, active plate boundaries are thin red lines, and extinct mid-ocean ridges are outlined as thin black lines; spherical polar stereographic projection.

maximum due to the high frequency of the GI air gun source. However, the sediment/basement contact is well identifiable in both lines and the stratigraphic relationships between the main seismic units on line B-B′ are clearly visible, allowing a tie with DSDP Site 274.

3. Seismic Well Tie

[5] The tie between the seismic lines and DSDP Site 274 is based on linking the NBP9702 Adare Trough seismic profiles with DSDP Site 274 via Eltanin seismic line ELT 52 (Figure 5). Drill hole DSDP 274 is located approximately 250 km northwest of Cape Adare [*Hayes et al.*, 1975]. From the 415 m of recovered sediment, six sedimentary, and five seismic units were identified and are summarized from *Keller* [2004] and *Hayes et al.* [1975]. The oldest dated sediments within the drill hole are the early Oligocene diatom rich detrital silty clays at the base of Unit 4 [*Hayes et al.*, 1975]. On the basis of regional magnetic models at the time [*Weissel and Hayes*, 1972] and extrapolation of sedimentation rates below the base of Unit 4, *Hayes et al.* [1975] suggested that the oldest sediments in the drill hole are likely early Oligocene or older. This is consistent with more recent magnetic data collected in the Adare Basin and in the Balleny Corridor NE of the Adare Basin [*Cande et al.*, 2000] that constrain the age of the ocean crust at DSDP 274 to be no older than early Oligocene (chron 13).

4. Seismic Units

4.1. Seismic Unit SU6

[6] The base unit is a nonporphyritic basalt containing white-green calcite veins, chlorite veins, and volcanic breccia. A distinct subbottom reflector marks the unit at approximately 0.50 sec below seafloor.

4.2. Seismic Unit SU5

[7] Eighty-seven meters of semilithified to lithified silty claystone correspond to this unit, which is separated from Seismic Unit SU4 by a strong reflection. Trace amounts of diatoms are present throughout, while porcellaneous chert is common in the upper section. These chert layers produce distinctive reflections, with seismically transparent layers above and below. Deposition occurred during the early Oligocene.

4.3. Seismic Unit SU3/4

[8] Lithologic Unit 4 from DSDP Site 274 averages about 150 m in thickness and corresponds

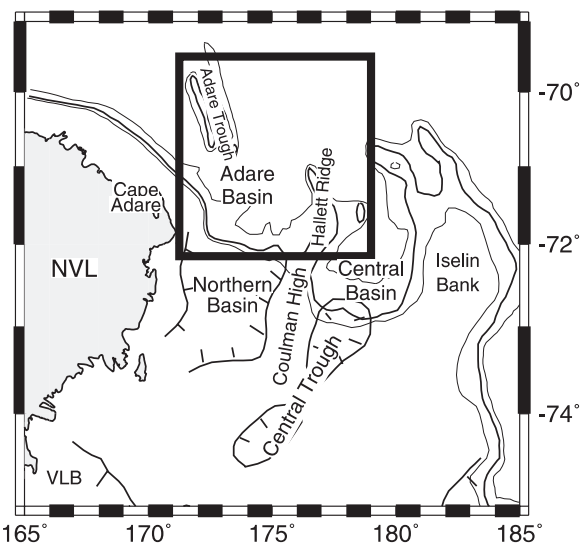

Figure 2. Main structural features of the Adare Trough area; inset map boundaries correspond to map frame of Figures 2 and 3; spherical Mercator stereographic projection. VLB, Victoria Land Basin; NVL, Northern Victoria Land.

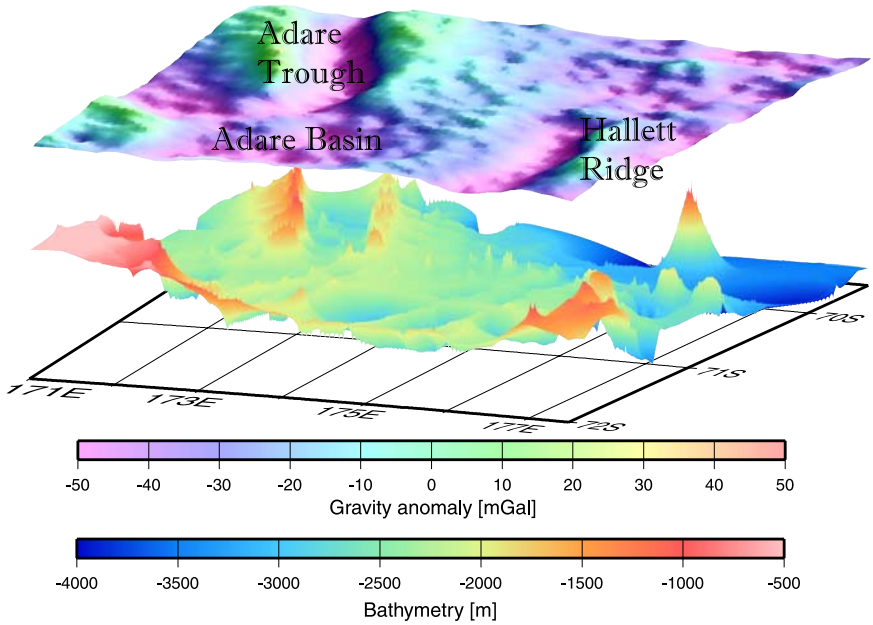

Figure 3. Perspective view of marine gravity anomalies from satellite altimetry from *McAdoo and Laxon* [1997] (top) and bathymetry of the Adare Trough and Basin area, based on merged multibeam data collected by the RV/IB N.B. Palmer in 1997 and regional single-beam ship bathymetry data; spherical polar stereographic projection.

to a highly uniform package of diatomaceous detrital silty clays to silty clay diatom oozes. Unit 4 is unconformably overlain by Unit 3, and this unconformity corresponds to a prominent reflection. Another well-expressed reflection within Unit 4 likely correlates to a zone of lithification seen in DSDP Site 274 downhole velocity measurements. The reflection corresponding to the unconformity between Units 3 and 4 is not regionally significant; therefore Units 3 and 4 are treated as a single seismic unit here that is referred to as SU3/4. The estimated age of this unit is middle-late Oligocene to early Oligocene.

4.4. Seismic Unit SU2

[9] Seismic Unit 2 corresponds to clay sediments in DSDP Site 274 with a yellowish-brown color, which is caused by the presence of ferromanganese oxides, and ferromanganese-coated pebbles and granules are present throughout the unit. The top of SU2 is defined by an unconformity. The unit is dated at mid-Miocene to the early Pliocene.

4.5. Seismic Unit SU1

[10] SU1 corresponds to a silty clay, deposited from the Pliocene to the Quaternary, with ice-rafted pebbles and granules, and diatoms, which are concentrated at the base of the unit.

5. Seismic Stratigraphy

[11] Figure 7 shows that units SU1-SU3/4 are laterally continuous from DSDP 274 to the intersection of ELT52 with NBP9702 Line B-B′. SU5 is the most readily identifiable unit in this seismic section. The contact between SU5 and SU3/4 is clearly defined by the transition between the characteristic reverberations from the chert in the upper part of SU5 and the relatively transparent package of diatom rich silty clays at the base of SU4. The sediment/basalt contact at the base of SU5 is also readily identifiable throughout the seismic section.

[12] Seismic units can be correlated from ELT52 to NBP9702 seismic line B-B′, and the identification of unconformities within the section provides good stratigraphic control on the location of seismic units. The unconformity between seismic units SU1 and SU2 is revealed at roughly 106 km in Figure 8 where reflections within SU2 are truncated at the base of SU1. At approximately 100–105 km reflections within SU3/4 onlap onto SU5 indicating that there was topography on the flanks of the Adare Trough at the time when the sediments of SU3/4 were deposited (Figure 8). Although seismic

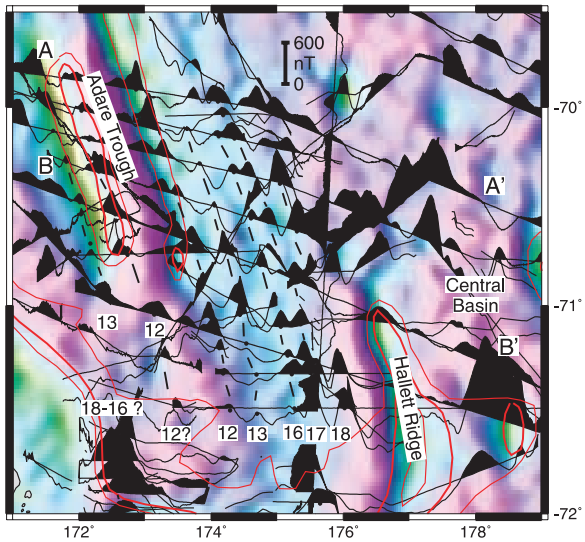

Figure 4. Marine magnetic anomalies in the Adare Trough/Basin area plotted as positive/negative wiggles along track overlain on gridded gravity anomalies from *McAdoo and Laxon* [1997] shown as color image (spherical Mercator projection). Magnetic anomalies (labeled) follow identifications by *Cande et al.* [2000]. The 1000, 1500 (heavy), and 2000 meter bathymetric contours (red lines) are also shown. The combined magnetic and gravity anomaly data illustrate that the Adare Trough is centered on an extinct spreading ridge, with magnetic anomaly 9 (not labeled) at its center. Note the asymmetry of magnetic lineations on either side of the extinct spreading ridge, resulting from asymmetric spreading, and the associated asymmetry of the Adare Trough, with a steeper and more severely uplifted rift flank on the slower spreading west side.

units outside of the central graben of the Adare Trough cannot be continuously traced across the bounding faults, the character of the seismic units and the locations of the unconformities are easily identifiable. The characteristic package of reflections from the chert layers at the top of Unit 5 is visible in the lower part of the sedimentary section within the trough. In the western part of the central graben, only the upper part of Unit 5 is inferred. At roughly 73–74 km (Figure 8), reflectors within SU3/4 are truncated at the base of SU2 and reflectors within SU1 onlap onto SU2, thus revealing the same geometry that is found on the East flank of the Adare Trough.

[13] Between 65 and 70 km on NBP9702 seismic line B-B′, there is a series of minor normal faults that step down toward the West. These faults clearly offset seismic units SU6-SU2; however SU1 appears to be relatively undisturbed. At 50–53 km (Figure 8), drag folding of SU5-SU2 is visible along the west bounding fault of the central graben of the trough (Figure 9). The reflections within SU1 are flat-lying, suggesting that motion along the bounding faults and minor faults within the trough ceased before the sediments of SU1 were deposited. On NBP9702 seismic line A-A′ (Figure 10), the data are of much lower quality than on seismic line B-B′, largely due to complications with the air guns and problems with the streamer due to bad weather conditions. Penetration along NBP9702 seismic line A-A′ is typically 0.5-1 second. An interpretation of seismic units as detailed as on profile B-B′ along this line is not possible; however this seismic line still provides some useful information. Along the eastern bounding fault, the uppermost seismic reflectors are flat lying while reflectors deeper in the section are drag folded along the fault. Deeper reflectors on the western bounding fault are also drag folded, but the uppermost layers are truncated at the seafloor near the west bounding fault. This is likely the result of local scouring by bottom water currents.

6. Inverting Mantle Bouguer Anomalies for Crustal Thickness

[14] To model Adare Trough crustal thickness and faulting, we use ship gravity data and the seismic

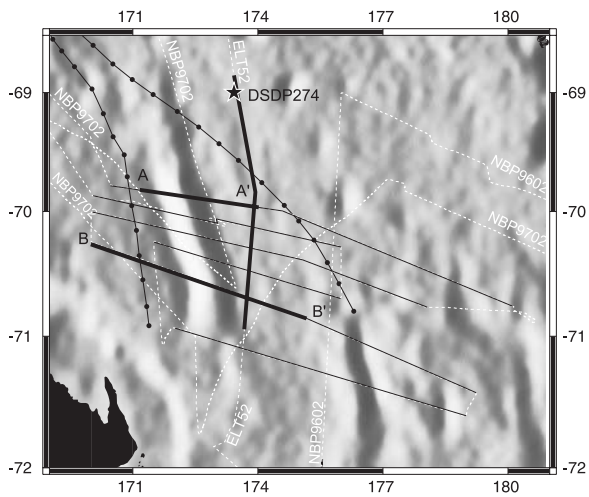

Figure 5. Mercator map of multibeam bathymetry lines collected on cruise NBP9702 aboard the RV/IB Nathaniel Palmer are shown by the thin black lines. NBP9702 and ELT 52 seismic lines shown in this paper are indicated with thick black lines. Other ship tracks are shown by dashed white lines, and the Adare triple junction trace, representing the boundary of the East-West Antarctic spreading center in the Adare Trough, is shown as a black-dotted line.

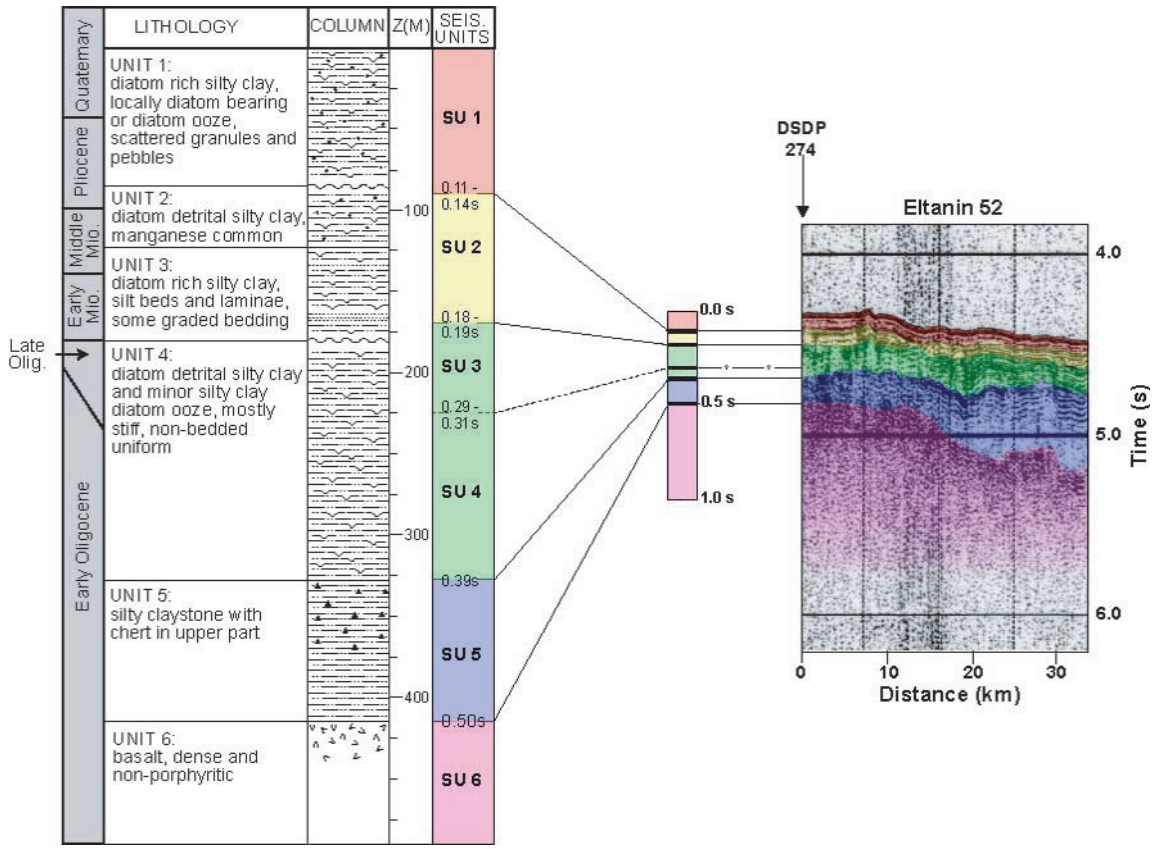

Figure 6. DSDP 274 stratigraphic column and correlation to ELT52 seismic line. Stratigraphic column after *Frakes* [1975] and *Hayes et al.* [1975]. Important seismostratigraphic markers include the package of reverberations off of chert layers at the top of SU5 as well as unconformities at the base of SU1 and SU2.

interpretation of profiles A-A′ and B-B′. Volcanic and igneous activity in the area is well expressed in profile B-B′, highlighting the ubiquitous intrusions in the Adare Trough and Basin areas, some of which penetrate the most recent sediments or form volcanic cones. This raises the possibility that the widespread intrusions in the Adare Trough/Basin area are rift-related, and that rift-flank uplift of the Adare Trough substantially postdates cessation of spreading.

[15] Our primary aim is to determine whether rift-flank faulting occurred soon after the cessation of seafloor spreading (i.e., in young lithosphere) or substantially later. To elucidate regional variations in crustal structure, we compute mantle Bouguer anomalies along the two seismic reflection profiles crossing the extinct ridge, based on a modeled Moho that is derived from the basement topography smoothed with a Gaussian filter with half-power point wavelength of 15 km, and an assumed average oceanic crustal thickness of 7 km [*White et al.*, 1992] (Figure 11). We find large positive mantle Bouguer anomalies (MBA) on profiles A-A′ and B-B′, with widths from 35–30 km and peak/trough amplitudes of 80–90 mGal (Figure 11). This is similar to what is observed at some other extinct ridges [*Jonas et al.*, 1991; *Jung and Vogt*, 1997].

[16] Mantle Bouguer anomalies indicate changes in crustal thickness or density, or the presence of a gabbroic root underneath the extinct ridge [*Jonas et al.*, 1991]. If we assume that mantle Bouguer anomalies are caused by undulations of a density contrast at the Moho, then we can use *Parker*'s [1973] method to invert the MBA for the Moho topography by downward continuing the low-pass filtered MBA. Water, crustal, lithospheric and asthenospheric densities are assumed to be constant (ρ_w = 1030 kg m^{-3}; ρ_c = 2800 kg m^{-3}; ρ_m = 3300 kg m^{-3}; ρ_a = 3179 kg m^{-3}). We apply a smoothing spline filter to stabilize downward continuation [*Müller and Smith*, 1993], which minimizes the Moho curvature, similar to

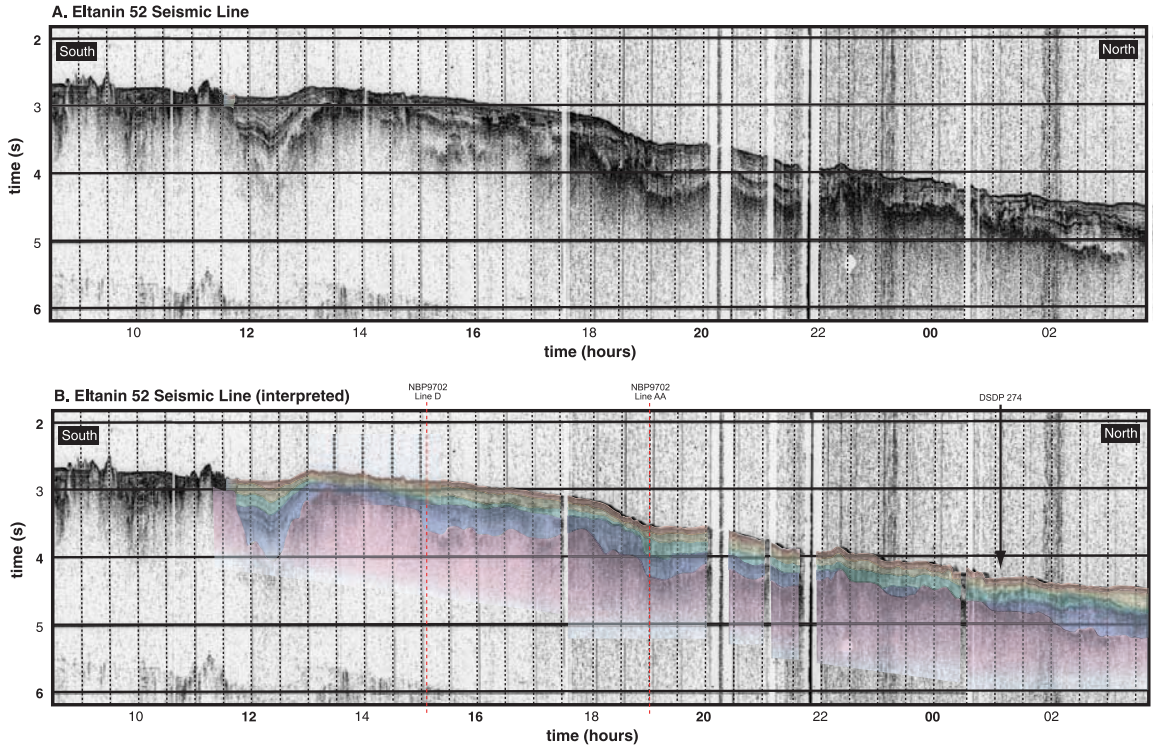

Figure 7. ELT52 analog seismic profiler record. This line shallows to the south as it rises up onto the flank of the Adare Trough. Seismic units correlated to DSDP hole 274 can be traced to the intersection with NBP9702 lines A-A′ and B-B′ (shown by the red dashed line).

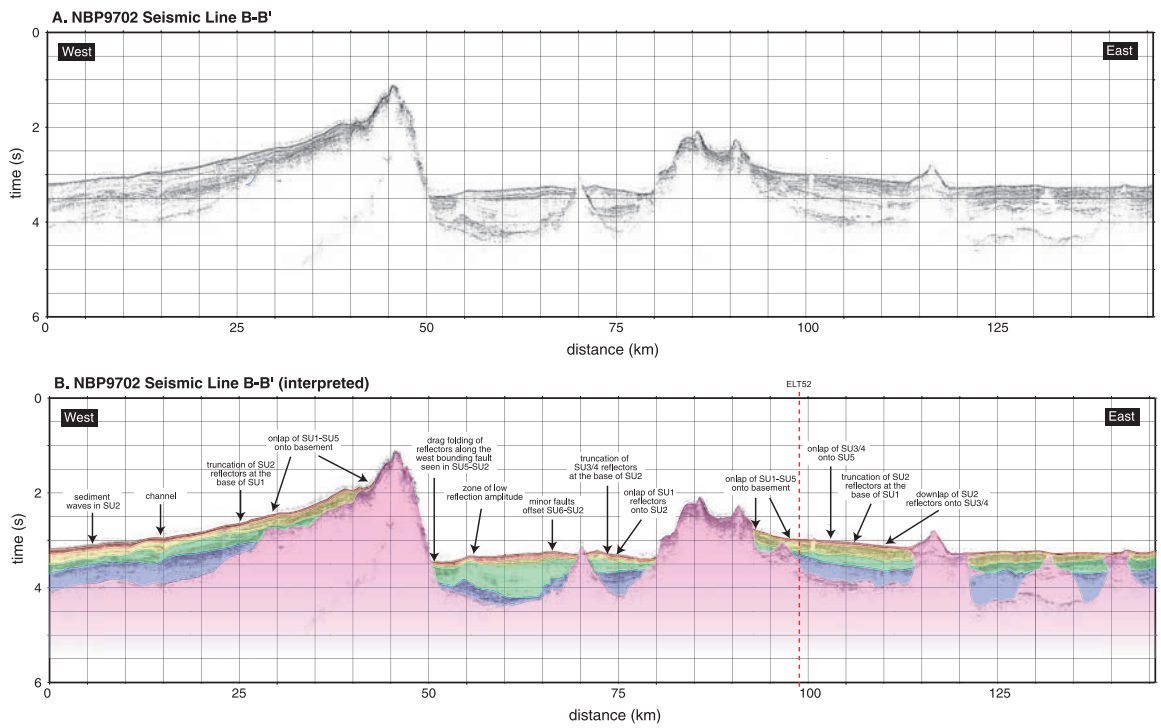

Figure 8. Uninterpreted and interpreted migrated seismic 48-channel profile (labeled B-B′ in Figure 4) of the Adare Trough. NBP9702 line B-B′ 48-channel migrated section. The vertical red dashed line indicates the intersection with the ELT52 seismic line.

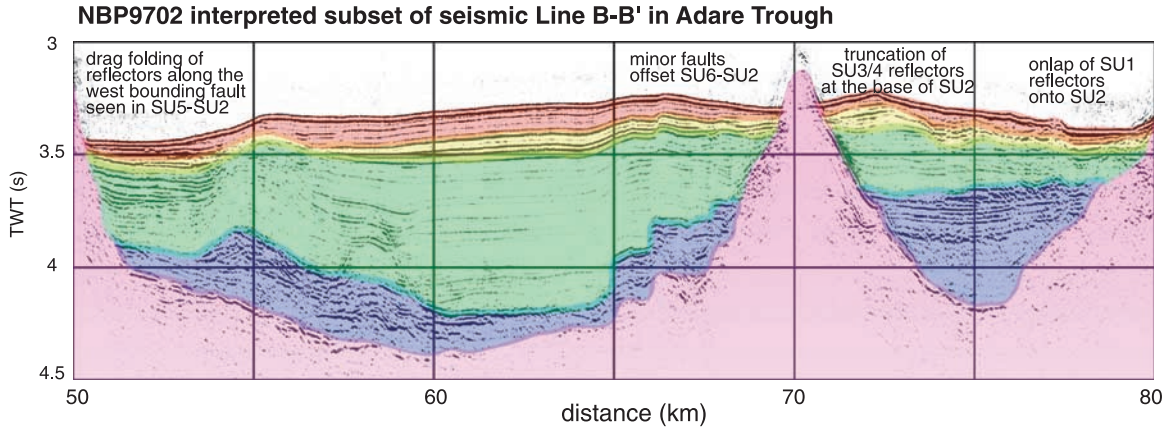

Figure 9. Interpreted subsection of profile B-B′ in the Adare Trough, highlighting the drag fold at the western flank of the Adare Trough and a minor fault postdating cessation of rifting between East and West Antarctica.

the procedure followed by *Phipps-Morgan and Blackman* [1993]. The filter is dependent on a characteristic wavelength λ chosen by the user. The larger λ, the smoother the Moho, and the larger the RMS misfit between the modeled and observed gravity anomaly. The suitable smoothing wavelength depends on the frequency content of the MBA. For the Adare Trough Moho models we chose to set λ to 60 km, after exploring a range of values, resulting in RMS misfits for modeled versus observed gravity anomaly profiles between 6.3 and 8.3 mGal (Figure 11). The classic tradeoff between modeled Moho resolution and variance in terms of the choice of lambda for this method is illustrated by *Müller and Smith* [1993].

[17] The modeled oceanic crustal thickness underneath the Adare Trough changes slightly southward from 10.5 km (A-A′) to 9 km (B-B′). The Adare Basin east of the Adare Trough shows the same trend, but with crustal thick-

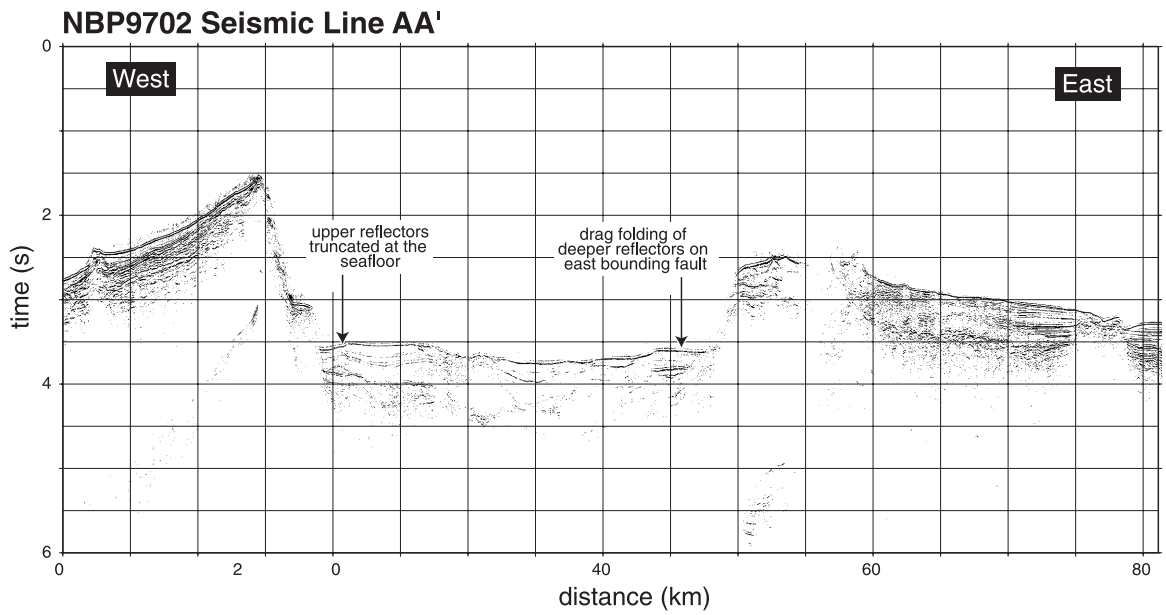

Figure 10. NBP9702 seismic line A-A′. Along the eastern bounding fault, the uppermost reflections are flat lying while reflections deeper in the section are drag folded along the fault. Deeper reflections along the western bounding fault are also drag folded. However, the uppermost layers are truncated at the seafloor near the fault, indicating local scouring due to bottom water current activity.

nesses of about 6 km along line A-A′ to 5 km at line B-B′ in the south. These results raise the question why the crust along the extinct ridge is anomalously thick.

[18] The modeled full spreading rates are virtually identical for the entire Adare Trough region both spatially and temporally [*Cande et al.*, 2000], and could therefore not have controlled changes in crustal thickness. The increased crustal thickness underneath the Adare Trough we observe is not just narrowly restricted to the inferred position of the extinct spreading center, but is rather about 100 km wide (Figure 11). Thus the spatial change in crustal thickness does not conform with that at the extinct Phoenix-Antarctic plate spreading ridge, where a reduction in spreading rate immediately prior to extinction may have caused a temporary magma oversupply, resulting in an increase in crustal thickness along a relatively narrow region along the extinct ridge [*Livermore et al.*, 2000]. Adare Trough half-spreading rates are extremely similar to the ultra-slow rates of the Eurasian Basin, where full spreading rates range from 6–13 mm/yr [*Jokat et al.*, 2003]. However, in the Eurasian Basin, crustal thickness decreased toward the Gakkel Ridge to minima between 1.9–3.3 km [*Jokat et al.*, 2003], contrary to our observations in the Adare Trough area.

[19] In order to further investigate the origin of crustal thickness variations in the Adare Trough area we use a new set of seafloor isochrons largely based on *Cande and Stock* [2005a] to produce a revised digital oceanic age grid for the southeast Indian and southwest Pacific oceans (Figure 12a). We use ETOPO5 bathymetry and sediment thickness grids (http://www.ngdc.noaa.gov/mgg/sedthick/sedthick.html) from NGDC (Figures 12b and 12c) to compute unloaded basement depth, using the relationship between sediment thickness and isostatic correction from *Sykes* [1996]. Predicted basement depth is then computed from the oceanic age grid using a thermal boundary layer depth-age model [*Parsons and Sclater*, 1977] (Figure 12e). The difference between predicted basement depth (Figure 12e) and unloaded basement depth (Figure 12d) yields residual basement depth (Figure 12f), which reveals a large regional positive residual depth anomaly between 1 and 2.5 km in amplitude, from offshore Victoria Land to the Balleny Islands and north of Iselin Bank. The origin of these depth anomalies may be partly dynamic, and partly due to crustal thickening. The Balleny Islands basement depth high is associated with an inferred heat flow anomaly up to 160 $mW/m^{2\cdot}$, based on the global seismic tomography-derived heat flow model by *Shapiro and Ritzwoller* [2004]. Upper mantle density images through time (Figure 13), based on the mantle convection model by *Steinberger et al.* [2004] as well as a synthesis from age and geochemistry data from the Cenozoic diffuse alkaline magmatic province (DAMP) in the southwest Pacific [*Finn et al.*, 2005] suggest that an major upper mantle thermal anomaly developed in the southwest Pacific in the last 50 million years.

[20] Therefore it is plausible that the mid/late Tertiary episode of slow spreading between East and West Antarctica was coupled with a mantle thermal anomaly, which may have been associated with a plume embedded in a larger-scale upwelling, increasing in amplitude toward the end of Adare Trough spreading, thus leading to the largest-amplitude crustal thickness anomaly in the youngest portion of the now extinct Adare spreading system. This idea is also supported by the volcanic and igneous activity in the Western Ross Sea and Marie Byrd Land since around 48 Ma [*Rocchi et al.*, 2002; *Tonarini et al.*, 1997]. The regional DAMP anomaly in the southwest Pacific area is known as embedding a multitude of small, relatively short-lived mantle plumes [*Clouard and Bonneville*, 2001], so the concepts of DAMP and plumes are not mutually exclusive. *Lizarralde et al.* [2004] found that crustal thickness decreases abruptly at half-spreading rates lower than about 15 mm/yr, and that the mechanism for the change is a reduction in melt extraction, rather than a reduction in melt production. This indicates that even if a magma over supply were present, it would not necessarily produce excess crust at the spreading rates modeled for the Adare Trough. The modeled crustal thickness anomaly underneath the extinct Adare Trough Ridge may instead reflect underplating; however, any interpretation in this regard will remain speculative unless the area is imaged in a seismic refraction experiment.

7. Modeling Rift Flank Uplift

[21] The uplift of rift flanks can be modeled as a flexural isostatic response to unloading of the lithosphere due to extension [*Weissel and Karner*, 1989]. We use the forward modeling approach

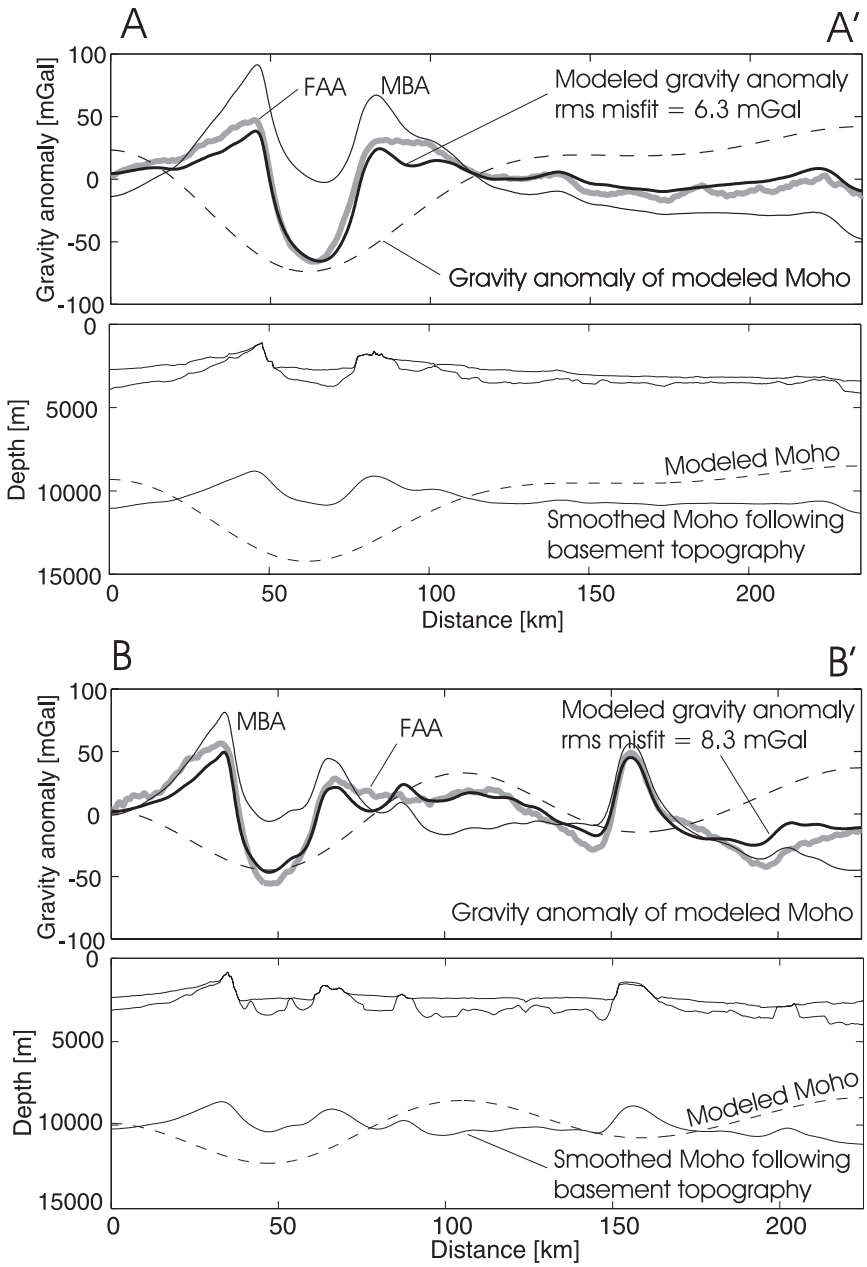

Figure 11. Simplified interpretations of seismic reflection profiles A-A′ and B-B′ (Figures 8 and 9). The basement depth was computed from two-way travel times based on an assumed average sediment velocity of 1.8 km/s. FAA, free air gravity anomaly; MBA, mantle Bouguer anomaly. Also shown is modeled Moho depth and the associated gravity anomaly from inverting the MBA based on a smoothing spline model (see text for discussion).

from *Weissel and Karner* [1989], based on the formation of a single extensional fault in oceanic crust, its associated flexural response and gravity anomaly, to individually model the uplift of the western and eastern flanks of the Adare Trough. The model output is compared to observed, unloaded basement topography and ship gravity anomalies. This model hinges on two critical concepts: (1) the lithosphere retains finite flexural rigidity (lateral strength) during extension and (2) the lithosphere is mechanically unloaded when normal slip occurs on a deeply penetrating fault resulting in isostatic rebound. If the lithosphere retains flexural rigidity during extension, the isostatic restoring stresses will be balanced by the deflection of a thin elastic plate. This isostatic response is dependent primarily on four variables: the effective elastic thickness (EET),

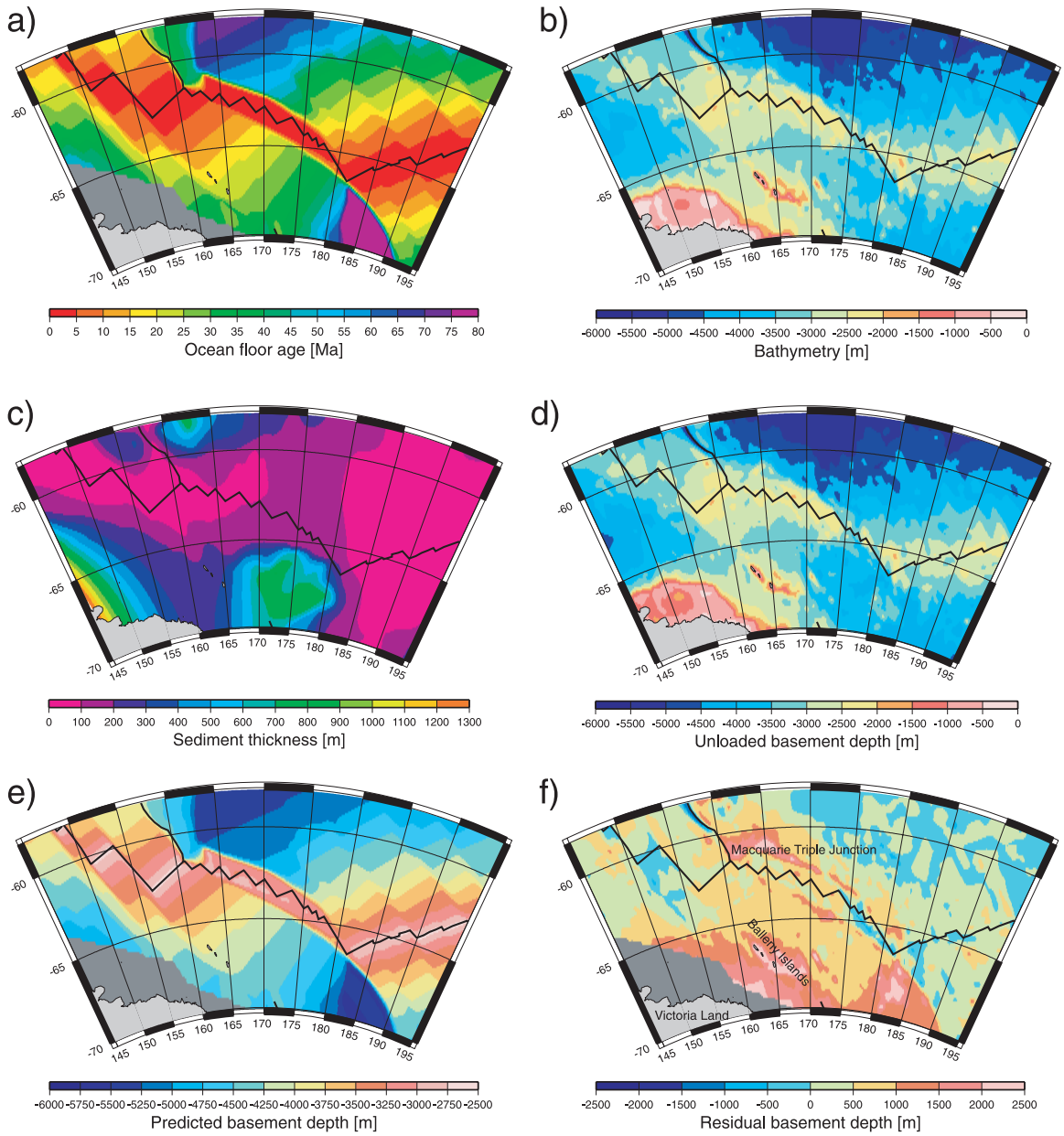

Figure 12. (a) Seafloor age, (b) bathymetry from etopo5, (c) sediment thickness from NGDC (http://www.ngdc.noaa.gov/mgg/sedthick/sedthick.html) [*Divins and Rabinowitz*, 1991; *Hayes and LaBrecque*, 1991; *Ludwig and Houtz*, 1979; *Matthias et al.*, 1988], (d) unloaded basement depth, (e) predicted basement depth from applying a thermal boundary layer depth-age relationship [*Parsons and Sclater*, 1977] to the seafloor age grid, and (f) residual depth grid obtained from subtracting Figure 12e from Figure 12d for the area north of the Adare Trough. Note large, regional positive depth anomaly northeast of Victoria Land. The southern limit of these maps is constrained by the southern extent of the NGDC sediment thickness grid.

the lithospheric thickness, the horizontal offset (heave) of the plate and the dip of the fault. The EET can be approximated as the depth to the 450°C isotherm (±150°C) [*Bodine et al.*, 1981].

[22] Our model includes the following assumptions: (1) The EET corresponds to the depth of the 450°C isotherm, and is identical on each side of the fault, (2) the lithospheric thickness corresponds to the depth of the 1300°C isotherm, and (3) water, crustal,

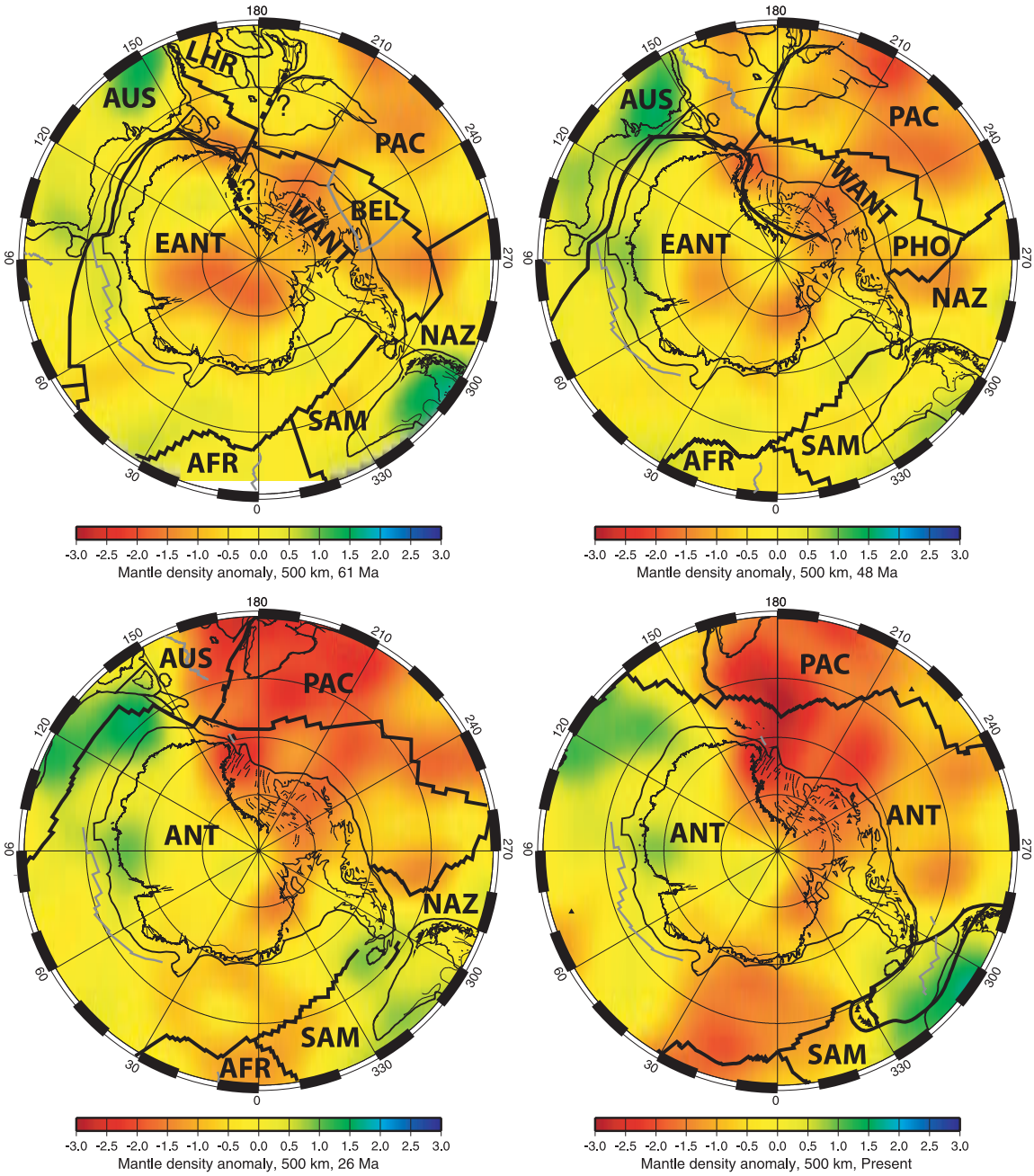

Figure 13. Plate reconstructions and locations of plate boundaries at chrons 27y (~61 Ma), 21o (~48 Ma), 8o (~26.5 Ma), and the present, overlain over mantle density anomaly at 500 km from *Steinberger et al.* [2004]. Nonclosure of the Pacific-West Antarctic-East Antarctic-Australian-Lord Howe Rise plate circuit during the opening of the Tasman Sea prior to 52 Ma requires a plate boundary either between the Lord Howe Rise and the Pacific Plate or between East and West Antarctica (dashed lines and question marks in 61 Ma reconstruction). At 26 Ma, East-West Antarctic extension ceases. Note the spreading of a mantle density anomaly in the southwest Pacific in the late Tertiary from 48 to 26 Ma, which further intensifies in the last 26 million years. This large-scale mantle upwelling, whose initiation has been interpreted as associated with an episode of slab breakthrough and mantle overturn [*Finn et al.*, 2005], may account for late Tertiary volcanism in Marie Byrd Land and the southwest Pacific in the absence of any major extension.

Table 1. Relationship Between Oceanic Lithospheric Age, Elastic Thickness (Approximated by the Depth of 450° Isotherm), and Lithospheric Thickness Based on a Cooling Halfspace Model for Selected Lithospheric Ages

	Lithospheric Age					
	25	20	15	10	5	3
Depth of 450° isotherm	10.0	9.0	7.5	6.0	4.7	3.4
Depth 1300° isotherm	75.0	67.5	58.0	48.0	34.0	16

lithospheric and asthenospheric densities are identical to those used above. We use the relationship between lithospheric temperature, elastic thickness and lithospheric age to estimate the age at which faulting occurred, by computing the flexural response of the oceanic lithosphere to normal faulting in terms of surface uplift and the associated gravity anomaly at six lithospheric ages from 3 to 25 million years (Table 1). Our model is based on the assumption of seafloor without any topography prior to the episode of faulting that created the Adare Trough. This is clearly an oversimplification; however, the basement topography adjacent to the Adare Trough, where it is not overprinted by younger magmatism (e.g., the western Adare Trough flank), displays only very minor basement roughness, justifying the application of a relatively simple flexural model.

[23] Fault dips were first measured on the seismic reflection profiles (Figures 8–10). Fault heave was estimated as the horizontal distance from the top of the outermost fault (flank) to the proximal edge of the trough, constituting the total horizontal movement arising from multiple faulting events over time. The western flank of the Adare Trough exhibits one major and at least one minor fault (Figure 8). As the summation of fault heaves is only a first approximation of the true heave, the measured heaves were adjusted during forward modeling to improve the fit between modeled and observed rift flank uplift and its associated gravity anomaly. The dip of the fault bounding the western Adare Trough flank averages 45°, whereas the eastern bounding fault dips 38° on average. The best-fit heave of the western fault is 4.5 km, whereas the eastern fault heave is about 3 km. The *Weissel and Karner* [1989] forward model was implemented in Matlab.

8. Discussion

[24] Figure 14 illustrates our model results, separated for western and eastern flank uplift. As the age of the lithosphere at the time of faulting is unknown, we explore a large range of possible lithospheric ages (3–25 million years). The isostatically rebounded model surface topography is compared with the observed, Airy-unloaded basement topography, using the sediment thickness from Figure 11. The model gravity anomaly, consisting of contributions from density contrasts at the Moho and the surface (seafloor) is compared with the observed free-air anomaly. The critical observations in this context are the decay or attenuation of either surface topographic uplift or the associated gravity anomaly away from the edge of the trough. Faulting in older, stronger lithosphere results in a more regionally uplifted, less steep rift flank with higher amplitude gravity anomalies due to the enhanced regional uplift of the Moho, as compared to faulting in younger lithosphere. Due to the pronounced mantle Bouguer anomaly across the Adare trough (Figure 11), it is not possible to achieve a good fit for both surface topographic uplift and the associated gravity anomaly. This is because *Weissel and Karner*'s [1989] model is not designed to take into account crustal thickness variations which existed prior to faulting. Noise is also introduced into the data due to the widespread magmatism/volcanism (Figures 8–10). However, despite these difficulties, it is clear that the models for faulting in 3 or 5 million years old lithosphere fit the observations substantially better than models for faulting in older lithosphere (Figure 14).

[25] The total amount of extension associated with Adare Trough normal faulting was about 7.5 km, and the effective elastic thickness (EET) at the time of faulting was between 3.5 and 5 km. This corresponds to a lithospheric age between 3 and 5 million years based on a thermal boundary layer model and assuming that the EET can be approximated by the depth to the 450° isotherm. This is a maximum age estimate considering that other slowly spreading ridges (e.g., the Carlsberg Ridge) have been shown to have an EET of at least 5 km near the zero-age ridge crest [*Ashalatha and Singh*, 2001; *Radha*, 1996]. Our results support a model in which the Adare Trough formed soon after spreading between East and West Antarctica became extinct, probably reflecting the final phase of extension before the two Antarcticas were united to form one plate. Therefore the age of the morphological Adare Trough structure clearly postdates the cessation of spreading.

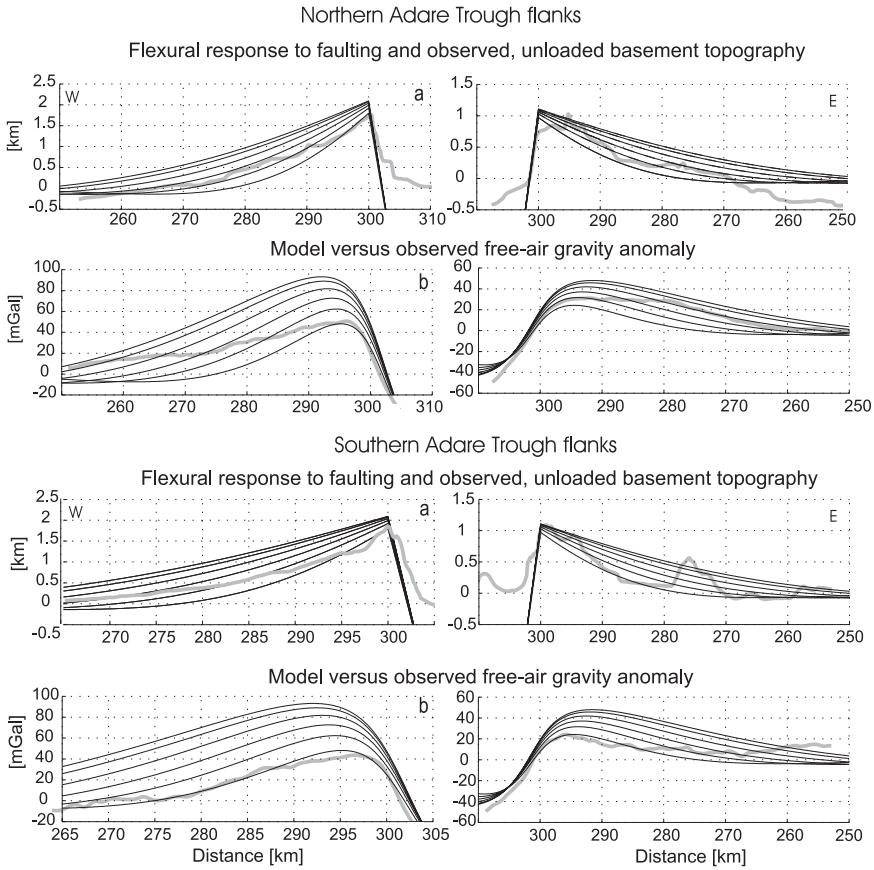

Figure 14. Rift-flank uplift models for western and eastern flanks of the Adare Trough, for model lithospheric ages of 3, 5, 10, 15, 20 and 25 million years (thin black lines, from bottom to top). Model outputs include (a) surface topography uplift and (b) gravity anomalies, superimposed over (a) observed airy-unloaded basement topography and (b) observed ship gravity anomalies as thick gray lines. See text for model parameters.

[26] Our analysis of available geophysical data in the Adare Trough area suggests that the mid/late Tertiary episode of slow spreading between East and West Antarctica was associated with a mantle thermal anomaly. The increasing crustal thickness toward the extinct ridge (Figure 11) indicates that this thermal mantle anomaly may have increased in amplitude through time during the Adare spreading episode. Our modeled crustal thickness anomaly is supported in a regional context by the residual basement depth anomaly from offshore Victoria Land to the Balleny Islands and north of Iselin Bank (Figure 12). This scenario is supported by a mantle convection model, which indicates the formation and strengthening of a major regional negative upper mantle density anomaly in the southwest Pacific in the last 50 million years [*Finn et al.*, 2005; *Steinberger et al.*, 2004]. There is little evidence for major subsequent structural activity in the Adare trough area from the available seismic data (Figures 8–10), indicating that this part of the West Antarctic Rift system became largely inactive in the early Miocene, with the exception of minor structural reactivation which is visible in the seismic data as offsets up to end of SU2 (early Pliocene).

9. Driving Forces of Extension Between East and West Antarctica

[27] To investigate the potential driving forces for East-West Antarctic rifting and volcanism, we plot the evolving plate boundary configuration around Antarctica over modeled mantle densities at 500 km depth from *Steinberger et al.*'s [2004] global analytical flow model. Compared to the Late Cretaceous, around 100 Ma, when the lower portion of the upper mantle underneath West Antarctica was still dominated by cold, subducted slab material [*Finn et al.*, 2005], *Steinberger et al.*'s [2004] model predicts the formation of a roughly linear, regional mantle upwelling in the lower upper mantle at 500 km depth in the early Tertiary at around

61 Ma, reaching from Victoria Land to the Bellingshausen Sea (Figure 13). The mantle convection model indicates that the regional upwelling at 61 to 48 Ma consisted of three centers, one underneath Victoria Land, one underneath West Antarctica and one centered at the triple junction between the Pacific, Nazca and Antarctic plates (Figure 13). A modeled transient negative upper mantle density anomaly underneath East Antarctica at 61 Ma is strongly diminished in amplitude and lateral extent at 48 Ma (Figure 13). If it existed, it appears to have had little effect on surface tectonics or magmatism. However, the negative density anomaly from Victoria Land to the Bellingshausen Sea increases in amplitude from 61 to 48 Ma (Figure 13), leading to the suggestion that increasing mantle driven surface uplift coinciding with a global tectonic reorganization at chron 21 (48 Ma) may have helped trigger East-West Antarctic extension along a preexisting line of weakness. Exactly how this anomaly continued to shallower depths in the upper mantle cannot be discerned from these models, as the mantle convection history is dependent on internal density heterogeneities derived from the global tomographic model by *Becker and Boschi* [2002], using a conversion factor of 0.25 only for data from below 220 km. The resulting mantle flow field through time, driven by mantle density anomalies and surface plate velocities, is only robust for the lower mantle and lower portion of the upper mantle. However, this scenario is consistent with the onset of magmatism at 48 Ma in Victoria Land [*Rocchi et al.*, 2002]. The mantle density anomaly images at 500 km depth also graphically demonstrate the tremendous expansion of the regional depth anomaly in the late Tertiary from 26 Ma to the present, postdating the cessation of East-West Antarctic rifting, and coinciding with the contemporaneous young volcanism in Marie Byrd Land, Thurston Island and Peter I Island, which can neither be attributed to rifting nor to a classical mantle plume [*Finn et al.*, 2005].

10. Conclusions

[28] The West Antarctic rift system is widely described as one of the largest active rift systems on Earth [*Behrendt*, 1999]. Recently, the existence of an active rift system in West Antarctica has been called into question on the basis of the observed pattern of seismicity [*Winberry and Anandakrishnan*, 2003] and GPS studies in West Antarctica [*Donnellan and Luyendyk*, 2004]. Our results support these conclusions. There is little evidence for major structural activity in the Adare trough area postdating rift-flank faulting and uplift, indicating that this part of the West Antarctic Rift system became largely inactive in the early Miocene. Observations regarding anomalously shallow basement depth and the mantle thermal history north of the Adare Trough area, suggest that Adare Trough spreading was associated with a mantle thermal anomaly, which increased in amplitude toward the late Tertiary.

Acknowledgments

[29] This work was supported by National Science Foundation grants NSF OPP 0126334 (to Stock) and OPP-01-26340 (to Cande) and by an Australian Research Council IREX grant (to Müller). We thank Bernhard Steinberger for providing outputs from his mantle convection model published in *Steinberger et al.* [2004]. Two anonymous reviews improved the quality of the paper substantially.

References

Ashalatha, B., and R. N. Singh (2001), Effects of fluid circulation on the thermal structure of evolving lithosphere: Application to Carlsberg Ridge, *J. Geol. Soc. India*, *58*, 351–359.

Becker, T., and L. Boschi (2002), A comparison of tomographic and geodynamic mantle models, *Geochem. Geophys. Geosyst.*, *3*(1), 1003, doi:10.1029/2001GC000168.

Behrendt, J. C. (1999), Crustal and lithospheric structure of the West Antarctic Rift system from geophysical investigations: A review, in *Lithosphere Dynamics and Environmental Change of the Cenozoic West Antarctic Rift System*, edited by F. M. Van Der Wateren and S. A. P. L. Cloetingh, *Global Planet. Change*, *23*, 25–44.

Bodine, J. H., M. S. Steckler, and A. B. Watts (1981), Observations of flexure and rheology of the oceanic lithosphere, *J. Geophys. Res.*, *86*, 3695–3707.

Cande, S. C., and J. M. Stock (2005a), Cenozoic reconstructions of the Australia-New Zealand-South Pacific sector of Antarctica, in *The Cenozoic Southern Ocean: Tectonics, Sedimentation and Climate Change Between Australia and Antarctica*, *Geophys. Monogr. Ser.*, vol. 151, edited by N. F. Exon et al., pp. 5–18, AGU, Washington, D. C.

Cande, S. C., and J. M. Stock (2005b), Constraints on the timing of extension in the Northern Basin, Ross Sea, paper presented at 9th International Symposium on Antarctic Earth Sciences, ISAES IX, Sci. Comm. on Antarct. Res., Potsdam, Germany.

Cande, S. C., J. M. Stock, R. D. Mueller, and T. Ishihara (2000), Cenozoic motion between East and West Antarctica, *Nature*, *404*, 145–150.

Clouard, V., and A. Bonneville (2001), How many Pacific hotspots are fed by deep-mantle plumes?, *Geology*, *29*, 695–698.

Divins, D. L., and P. D. Rabinowitz (1991), Total sediment thickness map for the South Atlantic Ocean, in *International Geological and Geophysical Atlas of the Atlantic and Pacific Oceans (GAPA)*, edited by G. B. Udintsev, pp. 147–148, Intergov. Oceanogr. Comm., Paris.

Donnellan, A., and B. P. Luyendyk (2004), GPS evidence for a coherent Antarctic plate and for postglacial rebound in Marie Byrd Land, *Global Planet. Change*, *42*, 305–311.

Finn, C. A., R. D. Müller, and K. S. Panter (2005), A Cenozoic diffuse alkaline magmatic province (DAMP) in the southwest Pacific without rift or plume origin, *Geochem. Geophys. Geosyst.*, *6*, Q02005, doi:10.1029/2004GC000723.

Frakes, L. A. (1975), Paleoclimatic significance of some sedimentary components at Site 274, *Initial Rep. Deep Sea Drill. Proj.*, *28*, 785–787.

Hayes, D. E., and J. L. LaBrecque (1991), Sediment isopachs: Circum-Antarctic to 30°S, in *Marine Geological and Geophysical Atlas of the Circum-Antarctic to 30°S*, *Antarct. Res. Ser.*, vol. 54, edited by D. E. Hayes, pp. 29–33, AGU, Washington, D. C.

Hayes, D. E., et al. (1975), Site 274, *Initial Rep. Deep Sea Drilling Proj.*, *28*, 369–433.

Jokat, W., O. Ritzmann, M. C. Schmidt-Aursch, S. S. Drachev, S. Gauger, and J. H. Snow (2003), Geophysical evidence for reduced melt production on the Arctic ultraslow Gakkel mid-ocean ridge, *Nature*, *423*, 962–965.

Jonas, J., S. A. Hall, and J. F. Casey (1991), Gravity anomalies over extinct spreading centers: A test of gravity models of active centers, *J. Geophys. Res.*, *96*, 11,759–11,777.

Jung, W. Y., and P. R. Vogt (1997), A gravity and magnetic anomaly study of the extinct Aegir Ridge, Norwegian Sea, *J. Geophys. Res.*, *102*, 5065–5089.

Keller, W. R. (2004), Cenozoic plate tectonic reconstructions and plate boundary processes in the Southwest Pacific, Ph.D. thesis, 129 pp., Calif. Inst. of Technol., Pasadena, Calif.

Livermore, R., et al. (2000), Autopsy on a dead spreading center: The Phoenix Ridge, Drake Passage, Antarctica, *Geology*, *28*, 607–610.

Lizarralde, D., J. B. Gaherty, J. A. Collins, G. Hirth, and S. D. Kim (2004), Spreading-rate dependence of melt extraction at mid-ocean ridges from mantle seismic refraction data, *Nature*, *432*, 744–747.

Ludwig, W. J., and R. E. Houtz (1979), Isopach map of the sediments in the Pacific Ocean basin, Am. Assoc. Pet. Geol., Tulsa, Okla.

Matthias, P. K., P. D. Rabinowitz, and N. Dipiazza (1988), Sediment thickness map of the Indian Ocean, *Map 505*, Am. Assoc. Pet. Geol., Tulsa, Okla.

McAdoo, D., and S. Laxon (1997), Antarctic tectonics: Constraints from an ERS-1 satellite marine gravity field, *Science*, *276*, 556–560.

Müller, R. D., and W. H. F. Smith (1993), Deformation of the oceanic crust between the North American and South American plates, *J. Geophys. Res.*, *98*, 8275–8291.

Parker, R. L. (1973), The rapid calculation of potential anomalies, *Geophys. J. R. Astron. Soc.*, *31*, 447–455.

Parsons, B., and J. G. Sclater (1977), An analysis of the variation of ocean floor bathymetry and heat flow with age, *J. Geophys. Res.*, *82*, 803–827.

Phipps-Morgan, J., and D. K. Blackman (1993), Inversion of combined gravity and bathymetry data for crustal structure: A prescription for downward continuation, *Earth Planet. Sci. Lett.*, *119*, 167–179.

Radha, K. M. (1996), Isostatic response of the Central Indian Ridge (western Indian Ocean) based on transfer function analysis of gravity and bathymetry data, *Tectonophysics*, *257*, 137–148.

Rocchi, S., P. Armienti, M. D'Orazio, S. Tonarini, J. R. Wijbrans, and G. Di Vincenzo (2002), Cenozoic magmatism in the western Ross Embayment: Role of mantle plume versus plate dynamics in the development of the West Antarctic Rift System, *J. Geophys. Res.*, *107*(B9), 2195, doi:10.1029/2001JB000515.

Shapiro, N. M., and M. H. Ritzwoller (2004), Inferring surface heat flux distributions guided by a global seismic model: Particular application to Antarctica, *Earth Planet. Sci. Lett.*, *223*, 213–224.

Steinberger, B., R. Sutherland, and R. J. O'Connell (2004), Prediction of Emperor-Hawaii seamount locations from a revised model of global plate motion and mantle flow, *Nature*, *430*, 167–173.

Sykes, T. J. S. (1996), A correction for sediment load upon the ocean floor: Uniform versus varying sediment density estimations—Implications for isostatic correction, *Mar. Geol.*, *133*, 35–49.

Tonarini, S., S. Rocchi, P. Armienti, and F. Innocenti (1997), Constraints on timing of Ross Sea rifting inferred from Cainozoic intrusions from Northern Victoria Land, Antarctica, in *The Antarctic region: Geological Evolution and Processes; Proceedings of the VII International Symposium on Antarctic Earth Sciences*, edited by C. A. Ricci, pp. 511–521, Terra Antarct., Siena, Italy.

Weissel, J. K., and D. E. Hayes (1972), Magnetic anomalies in the southeast Indian Ocean, *Antarct. Res. Ser.*, *19*, 165–196.

Weissel, J. K., and G. D. Karner (1989), Flexural uplift of rift flanks due to mechanical unloading of the lithosphere during extension, *J. Geophys. Res.*, *94*, 13,919–13,950.

White, R. S., D. McKenzie, and R. K. O'Nions (1992), Oceanic crustal thickness from seismic measurements and rare earth element inversion, *J. Geophys. Res.*, *97*, 19,683–19,715.

Winberry, J. P., and S. Anandakrishnan (2003), Seismicity and neotectonics of West Antarctica, *Geophys. Res. Lett.*, *30*(18), 1931, doi:10.1029/2003GL018001.